

Photorefractive effect and photoinduced quadratic nonlinear susceptibility in germanosilicate fibres fabricated in nitrogen and helium atmospheres by the MCVD technique

S A Vasil'ev, N N Vechkanov, E M Dianov, A N Gur'yanov, V M Mashinskii,
O I Medvedkov, O D Sazhin, V F Khopin, Yu P Yatsenko

Abstract. Single-mode optical fibres were fabricated from a germanosilicate glass by the method of modified chemical vapour deposition (MCVD), which used sintering of a porous glass in a reducing (helium or nitrogen-containing) atmosphere. The optical fibres exhibit a high photoinduced change in the refractive index and a high efficiency of recording quadratic nonlinear susceptibility compared to a standard germanosilicate fibre. Sintering, both in nitrogen and in helium atmospheres, was shown to increase the concentration of germanium oxygen-deficient centres in glass. It is likely that nitrogen enters into a germanosilicate glass in the concentration that is sufficient to modify the glass structure and to additionally increase its photosensitivity. The replacement of oxygen or silicon in the close vicinity of an oxygen vacancy by nitrogen may play a key role in the photosensitivity enhancement owing to the formation of additional valence bonds and blocking of recombination processes.

1. Introduction

As was shown recently in Refs [1–3], the doping of a germanosilicate glass with nitrogen in the thin-film technology and the technology of surface plasma chemical vapour deposition (SPCVD) of optical fibres increases its photosensitivity. It seems interesting to use these specific features in the modified chemical vapour deposition (MCVD) technique, which is extensively used for the fabrication of optical fibres.

However, in the MCVD process, the oxidation of silicon and germanium chlorides, the deposition of oxides in the form of highly dispersed amorphous silica, and its sintering to form a monolithic glass occur at considerably higher temperatures than in the plasma chemical technology. This prevents doping of germanosilicate glass with nitrogen at the chloride oxidation stage.

Nevertheless, it is hoped that nitrogen may be advantageous at a later stage of the technological process. For instance, the addition of nitrogen into an atmosphere during preform sintering by the outer deposition from the gas phase (OVD) in [4] provided its concentration in glass as high as 0.004–0.008%. As a result, additional bands appeared in the absorption spectrum of the fibres fabricated from this preform.

It is known that germanium oxygen-deficient centres (GODCs) with the 242-nm absorption band exist in a germanosilicate glass, and their concentration depends on the conditions of glass synthesis. Specific features of the MCVD process, which are caused by the deposition of a mixture of silicon and germanium oxides inside a high-melting silica tube, lead to the deficiency of oxygen in a germanosilicate glass even for the excess of oxygen in the gas phase. In this case, the deficiency of oxygen is predominantly caused by germanium atoms. All other methods of vapour-phase glass synthesis give considerably lower GODC concentrations for the same germanium concentration. One of the ways of increasing GODC concentration and, maybe, modifying these centres in the MCVD process is to form an oxygen-deficient atmosphere in a support tube during the sintering of deposited layers and the preform collapse due to the replacement of oxygen with other gases, in particular, with nitrogen [5].

The study of the photorefractive effect and the photoinduced SHG in nitrogen-containing germanosilicate optical fibres may give us insight into the role of nitrogen in the modification of centres responsible for these effects. It is known [6, 7] that both of them are directly related to the presence of GODCs, whose photodestruction may either produce a change in refractive index Δn or form the quadratic nonlinear susceptibility $\chi^{(2)}$ depending on irradiation conditions. For the photorefractive effect, the relationship follows from typical conditions of irradiation at UV wavelengths that almost exactly coincide with maxima of absorption bands of GODCs at 242 and 330 nm. For the photoinduced SHG, the relationship is not so evident. Here, it is common to use high-power IR laser radiation at 1064 nm and 532-nm radiation, which determines a complex multiquantum character of interaction with GODCs.

In particular, as shown in Ref. [8], third ($\lambda = 355$ nm) and especially fourth ($\lambda = 266$ nm) harmonics produced in nonlinear processes caused by the cubic nonlinearity $\chi^{(3)}$ in an optical fibre, may be of primary importance in the excitation and photoionisation of GODCs. The difference of these kinds of UV radiation in intensity and wavelength may determine specific features of the action on GODCs and their decay

S A Vasil'ev, N N Vechkanov, E M Dianov, V M Mashinskii, O I Medvedkov,
O D Sazhin Fibre Optics Scientific Centre, General Physics Institute,
Russian Academy of Sciences, ul. Vavilova 38, 117769 Moscow, Russia
A N Gur'yanov, V F Khopin Institute of High-Purity Substances, Russian
Academy of Sciences, ul. Tropinina 49, 603600 Nizhnii Novgorod, Russia
Yu P Yatsenko D V Skobel'tsyn Institute of Nuclear Physics, M V
Lomonosov Moscow State University, Vorob'evy gory, 119899 Moscow,
Russia

Received 20 March, 2000

Kvantovaya Elektronika 30 (9) 815–820 (2000)

Translated by A N Kirkin; edited by M N Sapozhnikov

products for these two effects. In particular, the photorefractive effect was found to be related to the GeE' centre, which represents one of the GODC decay products [9]. As for the photoinduced SHG, the most reliable experimental fact is that this effect is related to the Ge(1) centres [10]. This offers promise for studying the influence of nitrogen on colour centres [Ge(1, 2) and GeE' centres].

In this work, we have produced for the first time preforms with a germanosilicate core (7% molar concentration of GeO_2), sintered and collapsed in nitrogen and helium atmospheres in the MCVD process, and drew single-mode optical fibres from them. The UV absorption spectra and the efficiency of recording Δn and $\chi^{(2)}$ determined for these optical fibres were compared with the corresponding characteristics for bulk germanosilicate samples and optical fibres fabricated by the ordinary MCVD technology.

2. Experimental

In the SPCVD process, germanium efficiently enters into glass in an excess of oxygen in a gas mixture, whereas doping with nitrogen requires the presence of oxygen-deficient conditions. Thus, simultaneous doping of silica glass with germanium and nitrogen is difficult to realise even in the SPCVD process. Because of this, in the MCVD process, a layer of porous glass of the core was deposited in a usual oxygen atmosphere, and its sintering and the collapse of a tubular preform into a rod were carried out in nitrogen or helium atmospheres. According to the data of X-ray microanalysis, the atomic concentration of nitrogen in the MCVD sample was lower than 0.1% (the limiting sensitivity of the method). As for helium, it is assumed to be virtually absent in glass processed in this way, and its role consists only in the formation of strong reducing conditions for the production of a fibre preform.

The bulk samples prepared for UV spectral measurements represented transverse cuts of preforms, and they were approximately 0.1 mm thick. The characteristics of single-mode optical fibres drawn from these preforms are presented in the Table 1. Fibres no. 738 and 746 had a considerably higher optical loss in comparison with fibre no. 723 (in particular, because of a higher concentration of OH groups), but this had no substantial effect on the results of experiments on photoinduced phenomena because the fibres used in them were shorter than 20 cm.

In the experiments on the photoinduced change of refractive index, single-mode optical fibres were exposed through their lateral surface, in a region approximately 1 cm long, to the 244-nm second harmonic of a cw Ar^+ laser. The dynamics of changes in refractive index under this irradiation was determined from the evolution of the transmission spectrum of the Mach–Zehnder interferometer formed by two long-period gratings recorded in these optical fibres [2].

The quadratic nonlinear susceptibility was recorded in fibre samples 20 cm long. For this purpose, we used a Q-switched and mode-locked Antares Nd : YAG laser (Coherent) emitting at 1064 nm. It produced 100-ps pulses with 1.2-kHz repetition rate. A pulse train had an envelope 200 ns long. Moreover, we injected into a fibre seeding radiation of the second harmonic at 532 nm. The efficiency of the gratings of quadratic nonlinear susceptibility, which was estimated from the ratio of powers of the photoinduced second harmonic and IR radiation, reached a maximum value of $\sim 1 - 2\%$.

When recording the $\chi^{(2)}$ grating, we also detected at the output of a fibre UV radiation at 266 nm, which corresponded to the fourth harmonic of IR radiation at 1064 nm. This radiation was measured with a monochromator. Photometric measurements showed a linear dependence of the 266-nm signal on the intensity of the second harmonic at 532 nm and its quadratic dependence on the intensity of IR radiation at 1064 nm [8]. In the case where the recording was carried out using a strong seeding radiation, the fluctuating signal at 266 nm was reliably observed by a photodetector from the beginning of $\chi^{(2)}$ grating formation. In the case of a weak seeding signal at 532 nm, the 266-nm signal was observed only at the final stage of the process, when the photoinduced second harmonic reached a sufficiently high power.

3. Results and discussion

3.1. UV absorption spectra of preforms

Fig. 1 presents UV absorption spectra for all the samples. One can clearly see in it the GODC absorption band at 242 nm and the short-wavelength absorption edge ($\lambda < 210$ nm). Note that the thickness of sample no. 746 was too large for the measurement of absorption near the maximum of the 242-nm band. The spectra of the MCVD samples no. 738 and 746 sintered in nitrogen or helium atmosphere where similar in shape to the spectrum of the standard germanosilicate glass (no. 723).

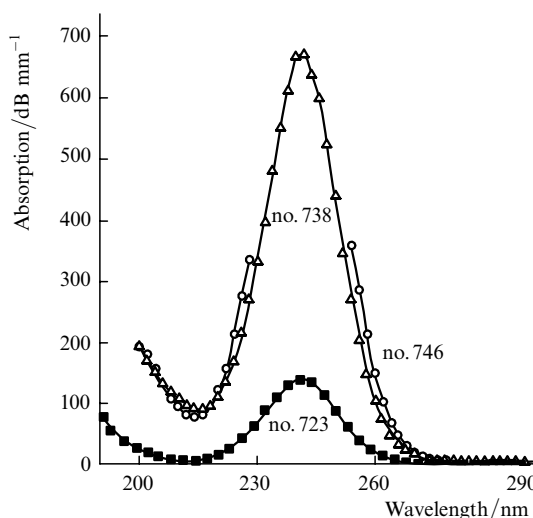


Figure 1. UV absorption spectra of bulk samples.

However, the absorption band of GODCs in these samples is higher in intensity than the band in the standard germanosilicate glass (see the Table 1). The absorption coefficient reduced to the GeO_2 molar concentration reaches almost $100 \text{ dB}(\text{mm } \%)^{-1}$ in preform no. 738 and about $135 \text{ dB}(\text{mm } \%)^{-1}$ in preform no. 746. These values exceed the absorption coefficients presented in Ref. [5] by a factor of two.

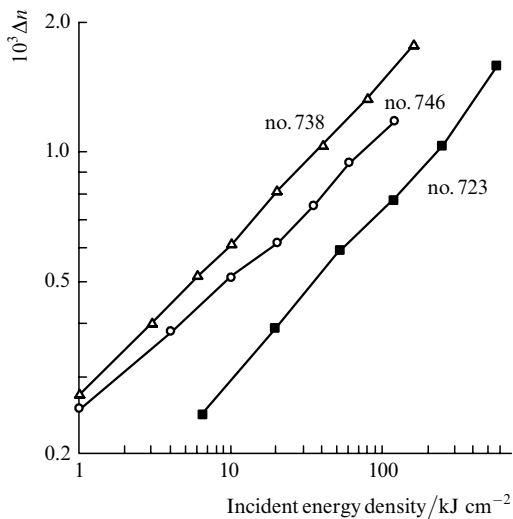
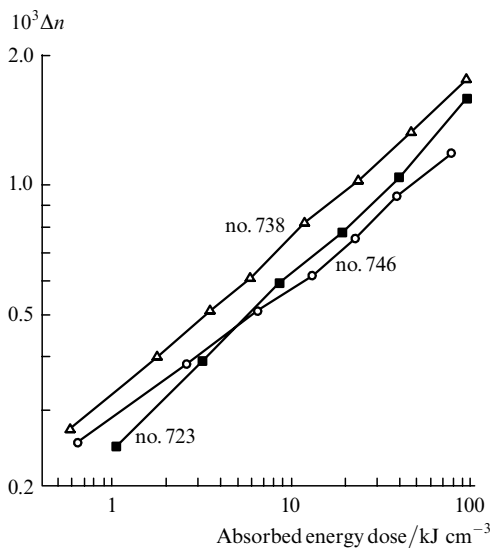
This difference is likely to be caused by the fact that we used the oxidising atmosphere both at the sintering stage and at the preform collapse stage. The absorption coefficient for the standard MCVD sample was $\sim 20 \text{ dB}(\text{mm } \%)^{-1}$. Thus, sintering in the nitrogen or helium atmosphere strongly increases the GODC concentration (by a factor of 5–7).

Table 1. Characteristics of experimental samples (preforms and single-mode fibres).

Sample number	Molecular concentration of GeO ₂ in the core/%	Atmosphere for sintering and collapse	Absorption coefficient at $\lambda = 242 \text{ nm}/\text{dB mm}^{-1}$	Absorption coefficient at $\lambda = 266 \text{ nm}/\text{dB mm}^{-1}$	Cutoff wavelength λ_c/nm
723	7	O ₂	140	6	925
738	7	N ₂ O	670	35	805
746	7	He	940 (estimate)	51	750

3.2. Photoinduced change of the refractive index in optical fibres

The dependence of the change in refractive index on the energy density of radiation incident on a fibre is presented in Fig. 2. One can see that the samples sintered in nitrogen or helium are characterised by a higher change in refractive index than the standard sample.

**Figure 2.** Dependence of the change in refractive index on the incident energy density.**Figure 3.** Dependence of the change in refractive index on the absorbed energy dose.

For the qualitative elucidation of the role of GODCs and other factors in photorefractive properties of germanosilicate glass, we estimated the portion of absorbed energy. For this purpose, we measured the radial distribution of GODC absorption at 242 nm and measured the absorption coefficient averaged over the cross section. The portion of absorbed energy, measured with respect to the radiation dose, was 7% for sample no. 723 and 28% for sample no. 746. Fig. 3 presents the dependence of the change in refractive index on the absorbed UV radiation dose for different samples. The MCVD sample sintered in helium (no. 746) showed approximately the same efficiency of photorefractive conversion of UV radiation absorbed by GODCs as the standard germanosilicate sample.

This means that in this case an increase in photosensitivity is totally caused by an increase in GODC concentration. At the same time, the efficiency of recording Δn in the nitrogen-containing samples remained higher by a factor of 1.5–2 even upon normalisation to absorbed energy. It is likely that nitrogen has an additional specific influence on the photorefractive effect in germanosilicate glass. One of the possible reasons consists in the fact that oxygen enters into the glass matrix rather close to GODCs. This suggests that nitrogen can have a double influence on the photoinduced reconstruction of GODCs.

(1) Within the framework of the model of GODC photoionisation, electron traps are of considerable importance. In pure germanosilicate glass, the major trap represents a four-coordinate germanium atom, which transforms upon electron capture into a Ge(1) centre. In this case, a GeE' centre remains at the place of an ionised GODC, and this centre is well known to be associated with the photorefractive effect [9]. However, Ge(1) centres have a rather low thermal- and photostability. They decay, most likely, through recombination with GeE' centres, and reconstruct GODCs.

In nitrogen-containing germanosilicate glass, a nitrogen atom introduced as a substitutional impurity into an oxygen ($\equiv \text{Si}-\text{N}-\text{Si} \equiv$) or a silicon (NO_4) site of an atomic matrix of silica glass may be an efficient and stable electron trap [11]. Thus, nitrogen can favour the formation of GeE' centres in higher concentration with a higher stability.

(2) Within the framework of the model of a neutral oxygen vacancy, the dominant contribution to the photorefractive effect is made by the relaxation of GODCs upon UV excitation to the so-called puckered state [12]. This state is stabilised due to the formation of a threefold coordinated oxygen atom in the glass matrix. The probability of this process is low and depends in a considerable extent on the arrangement of oxygen atoms from the surrounding of a defect. It is reasonable to assume that in the case of nitrogen-doped glass a polyvalent nitrogen atom is a more suitable stabiliser for a puckered silicon atom than the bridge oxygen, which enhances the photoinduced change in refractive index, the absorbed UV radiation doses being the same.

3.3. Quadratic nonlinear susceptibility $\chi^{(2)}$

Fig. 4 presents on the time scale the growth of gratings of quadratic nonlinear susceptibility for the optical fibres under study. They were obtained for fixed irradiation conditions. (The seeding radiation was switched off at the early stage of the recording process.) The grating amplitude is quantitatively characterised by $I_2/I_1^2 \sim (\chi^{(2)}L)^2$, where I_1 and I_2 are the peak intensities of IR radiation and the photoinduced second harmonic, respectively, and L is the effective length of the $\chi^{(2)}$ grating. The comparison of the efficiency of recording $\chi^{(2)}$ gratings for the curves presented in Fig. 4 with the efficiency of the change induced in the refractive index of the optical fibres under study by 244-nm radiation (Fig. 2) shows that these characteristics are correlated.

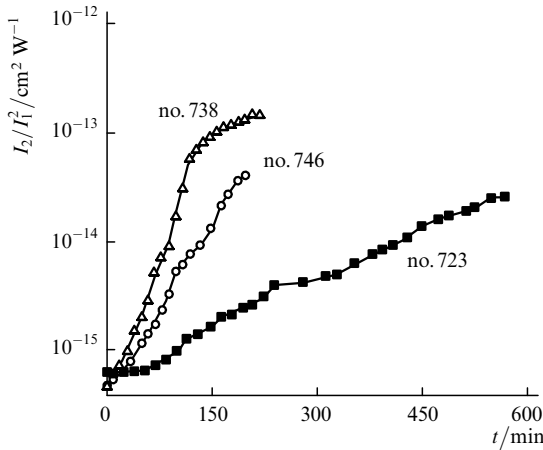


Figure 4. The growth of the $\chi^{(2)}$ grating in germanosilicate fibres in time for recording IR radiation with the peak power $P_1 = 21 - 22$ kW.

For both effects, the highest photosensitivity was observed for the nitrogen-doped germanosilicate optical fibre (no. 738). The optical fibre no. 746 had a higher GODC concentration than the nitrogen-doped fibre, but its photosensitivity was lower. In both cases, the lowest sensitivity was observed for the standard fibre no. 723. This correlation may be associated with the similarity of the action of radiation on one and the same GODCs having main absorption bands in the UV spectral region.

For the photorefractive effect, the character of excitation and photoionisation of GODCs and, therefore, the absorbed dose are uniquely determined by one- and two-quantum processes of 244-nm radiation absorption by the singlet band at 242 nm (Fig. 5a). In the case of the photoinduced effect, one should determine more precisely the radiation making the dominant contribution to the excitation of these centres when passing from the time dependences to similar dependence on the radiation dose. Here, we use the model proposed in Ref. [8], according to which the GODCs involved in the $\chi^{(2)}$ grating formation are excited by the UV radiation produced in the nonlinear process on the $\chi^{(3)}$ inside an optical fibre.

The removal of excitation from singlet (S_1) and triplet (T_1) levels, which leads to the photodestruction of GODCs, occurs through the interference of the two-quantum process for IR radiation and the one-photon process for its second harmonic (Fig. 5b). As shown in Ref. [8], in the case where IR radiation at 1064 nm and the seeding harmonic at 532 nm are used for recording the $\chi^{(2)}$ grating, the dominant

contribution to the excitation of GODCs is made by 266-nm radiation produced in the nonlinear processes based on $\chi^{(3)}$ ($4\omega = \omega + \omega + 2\omega$) and falling into the singlet absorption band of GODCs. When determining the dependences on doses, we used the intensities calculated for 266-nm radiation. (Note that it was difficult to make exact measurements of this intensity inside an optical fibre in the course of $\chi^{(2)}$ grating growth, especially for a weak seeding radiation.)

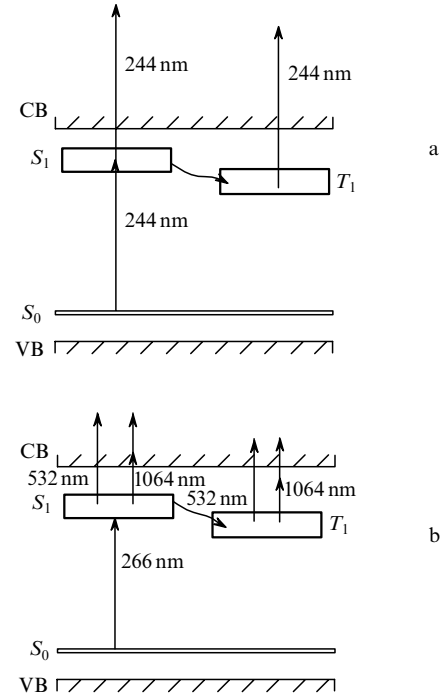


Figure 5. Diagrams of excitation and photoionisation of GODCs in the photorefractive effect (a) and the effect of photoinduced quadratic nonlinear susceptibility (b). (VB) valence band, (CB) conduction band.

The intensity was calculated by the expression

$$I_4(z) = \frac{16\omega^2 \mu_0^2 (\chi^{(3)})^2 I_1^2 I_2 \sin^2(\Delta kz/2)}{n_4 n_1^2 n_2} z^2,$$

which was obtained in the given-field approximation from the system of coupled equations for the nonlinear mixing of waves with frequencies 4ω , ω , and 2ω on $\chi^{(3)}$ ($4\omega = \omega + \omega + 2\omega$) [13]. Here, $I_4(z)$ is the peak intensity of the fourth harmonic of IR radiation ($\lambda = 266$ nm); z is the spatial coordinate along the fibre axis; ω is the IR radiation frequency; μ_0 is the absolute magnetic permeability; n_1 , n_2 , and n_4 are refractive indices of the fibre core at the frequency of IR radiation and its second and fourth harmonics, respectively; and $\Delta k = (2\omega/c)(2n_4 - n_1 - n_2)$. This relation was deduced taking into account the fact the coherence length $l_c = \pi/\Delta k \sim 3$ μm was much smaller than the absorption length $l_{\text{abs}} = 1/\alpha_{266}$ (for the refractive index α_{266} corresponding to the data in the table, $l_{\text{abs}} \geq 92$ μm).

The absorbed radiation dose at 266 nm was calculated under the assumption that the pulses had the Gaussian shape and duration $\tau_4 = \tau_1 \tau_2 / (2\tau_2^2 + \tau_1^2)^{1/2}$, where τ_1 and τ_2 are the pulse durations for IR radiation and its second harmonic. The average intensity was determined from the relation $\bar{I}_4 = \sqrt{\pi}/2 I_4 \tau_4 N$, where

$$\bar{I}_4 = (2\pi/\Delta k)^{-1} \int_0^{2\pi/\Delta k} I_4(z) dz$$

is the peak intensity averaged over the beating period $2\pi/\Delta k$ and N is the pulse repetition rate. Taking into account the fact that $l_c \ll l_{\text{abs}}$, the absorbed dose was determined as

$$E_{\text{abs}}(t) = [1 - \exp(-\alpha_{266} 2\pi/\Delta k)] / (2\pi/\Delta k) \int_0^t \bar{I}_4(t) dt \\ \approx \alpha_{266} \int_0^t \bar{I}_4(t) dt,$$

where t is the current time of $\chi^{(2)}$ grating recording.

The dependences of I_2/I_1^2 on the energy of 266-nm radiation produced inside a fibre and absorbed in a unit volume, calculated for the curves in Fig. 4, are presented in Fig. 6. These curves are similar in their basic features to the dependences for the photorefractive effect. In particular, it follows from them, like in the case of Δn recording, that the higher efficiency of $\chi^{(2)}$ grating recording in the fibre no. 746, which was produced in the helium atmosphere, in comparison with the standard germanosilicate fibre no. 723 (see Fig. 2 and Fig. 6a) is most likely associated with an increase in GODC concentration rather than with the modification of photocentres. At the same time, the MCVD fibre no. 738, produced in the nitrogen-containing atmosphere demonstrates in $\chi^{(2)}$ grating recording, similar to the Δn grating recording, an increased sensitivity in comparison with the standard fibre, the absorbed UV energy being fixed. This suggests that its photocentres are modified under the action of nitrogen.

Distinctions in the dependences on the radiation dose are associated with specific features of $\chi^{(2)}$ formation in optical fibres. Note that the UV radiation intensities at which the Δn and $\chi^{(2)}$ amplitudes saturate differ by three orders of magnitude. The amplitude of the photoinduced $\chi^{(2)}$ grating saturates at the absorbed dose somewhat above 10 J cm^{-3} , which corresponds to 10^{19} photon cm^{-3} for radiation at 266 nm.

The difference in dose may be associated with different roles of Ge(1) and GeE' centres in these effects. When the $\chi^{(2)}$ grating is formed, the Ge(1) centres are the major contenders to the role of negatively charged traps in its ordered charge structure. It is likely that the destruction of Ge(1) centres by 266-nm radiation falling into their absorption band at 281 nm [14] is the factor limiting the efficiency of $\chi^{(2)}$ grating recording.

As shown in Ref. [14], the saturation of concentration of Ge(1) centres in the case of exposure to 248-nm radiation, which is close in wavelength to the 244-nm radiation used for inducing Δn , is observed for a dose of 10^{20} photon cm^{-3} (100 J cm^{-3}). Nevertheless, at such doses, the dependences of Δn on the dose (Fig. 3) contain no specific features. This may give evidence of a considerably larger role of other GODC decay products in the photorefractive effect, in particular, of GeE' centres, which manifest a weaker tend to saturation at doses above 10^{20} photon cm^{-3} .

When elucidating the role of nitrogen, one should take into account the fact that the processes taking place at GeE' centres are also important for the formation of the charge structure of the $\chi^{(2)}$ grating. In the majority of the models of $\chi^{(2)}$ gratings that are based on charge separation, the positive charge produced through the decay of a neutral vacancy (a GODC) and conjugate to the negative charge of a germanium trap Ge(1) is assumed to be in the nearest surrounding of a GeE' centre.

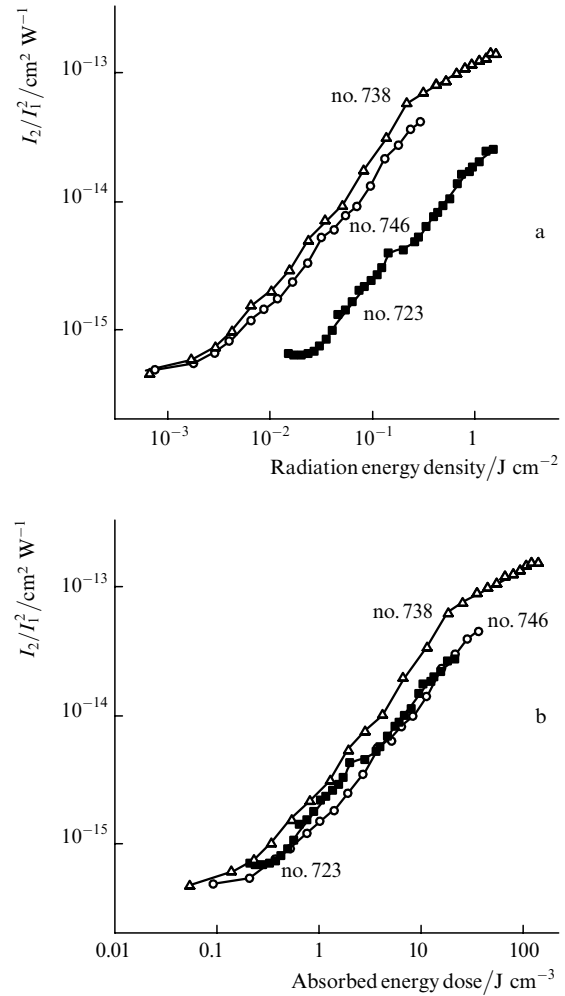


Figure 6. Dependences of the $\chi^{(2)}$ grating growth, calculated for the curves in Fig. 4, on the energy density of 266-nm radiation produced in optical fibres (a) and on the absorbed energy dose of this radiation (b).

Approximately the same influence of nitrogen at high and low radiation doses for these two effects suggests that it may be involved in the formation of complexes that primarily act on the surrounding of GeE' centres. In particular, the nitrogen structures formed by the substitution type reactions in oxygen or silicon sites and found in the first or in the second coordination sphere of the oxygen vacancy, respectively, may not only represent additional photoelectron traps in the photoionisation of GODCs, but also passivate the positive charge and hamper its recombination with a photoelectron due to the formation of additional bonds with GODC decay centres.

4. Conclusions

Using the MCVD method modified by sintering porous glass in an atmosphere containing nitrogen or helium, we produced single-mode fibres from a germanosilicate glass. The sintering in a reducing atmosphere increases the GODC concentration in glass. Moreover, it is likely that nitrogen enters into germanosilicate glass in the concentration that is sufficient for modifying the structure of glass and increasing its photosensitivity.

The correlation between the efficiencies of Δn and $\chi^{(2)}$ recording in such optical fibres and in the standard MOCVD

fibre was found. The fibres fabricated in the nitrogen atmosphere were shown to have a higher photosensitivity not only due to an increased concentration of GODCs, like in the case of the fibres produced in the helium atmosphere, but also due to the modification of their centres with participation of nitrogen.

We have obtained for the first time the dependences of the parameter I_2/I_1^2 , which characterises the $\chi^{(2)}$ grating amplitude, on the absorbed dose of 266-nm radiation produced in the nonlinear process involving $\chi^{(3)}$ ($4\omega = \omega + \omega + 2\omega$) inside an optical fibre. The absorbed 266-nm radiation doses required for $\chi^{(2)}$ saturation were found to be at least three orders of magnitude lower than the 244-nm radiation doses saturating Δn .

To elucidate the influence of nitrogen leading to an increase in the efficiency of both $\chi^{(2)}$ and Δn recording, one should primarily take into account the modification of the nearest surrounding of GeE' centres caused by polyvalent nitrogen atoms because they are likely to be closely related to both effects. In this case, the photosensitivity of glass is increased due to the formation of additional valence bonds and the blocking of recombination processes.

Acknowledgements. The authors thank S V Lavrishchev for the measurement of oxygen concentration and V B Neustruev for his critical remarks.

References

1. Poulse C V, Storgaard-Larsen T, Hubner J, Leistico O *Proc. SPIE Int. Soc. Opt. Eng.* **2998** 132 (1997)
2. Dianov E M, Golant K M, Mashinsky V M, Medvedkov O I, Nikolin I V, Sazhin O D, Vasiliev S A *Electron. Lett.* **33** 1334 (1997)
3. Dianov E M, Yatsenko Yu P *Kvantovaya Elektron. (Moscow)* **25** 262 (1998) [*Quantum Electron.* **28** 254 (1998)]
4. Gilliland J W, Powers D R *Electron. Lett.* **23** 144 (1987)
5. Dong L, Pinkstone J, Russel P St J, Payne D N *J. Opt. Soc. Am.* **11** 2106 (1994)
6. Awazu K, Hosono H, Kawazoe H *Proc. SPIE* **2044** 78 (1993)
7. Tsai T E, Friebele E J, Griscom D L *Proc. SPIE* **2044** 121 (1993)
8. Dianov E M, Kornienko L S, Yatsenko Yu P *Kvantovaya Elektron. (Moscow)* **23** 652 (1996) [*Quantum Electron.* **26** 636 (1996)]
9. Simmons K, La Rochelle S, Mizrahi V, Stegeman G, Griscom D *Opt. Lett.* **16** 141 (1991)
10. Gallagher M D, Osterberg U L *J. Appl. Phys.* **74** 2771 (1993)
11. Sulimov V B *Thesis for Doctor's Degree* (Moscow: General Physics Institute, Russian Academy of Sciences, 1997)
12. Sulimov V B, Sokolov V O, Dianov E M, Poumellec B *Phys. Status Solidi A* **158** 155 (1996)
13. Blombergen N *Nonlinear Optics* (New York: Benjamin, 1965)
14. Neustruev V B, Dianov E M, Kim V M, Mashinsky V M, Romanov M V, Guryanov A N, Khopin V F, Tikhomirov V A *Fibres Integrated Optics* **8** 143 (1989)